Fuel 166 (2016) 179–187

Contents lists available at ScienceDirect

Fuel

journal homepage: www.elsevier.com/locate/fuel

Novel effect of SO_2 on selective catalytic oxidation of slip ammonia from coal-fired flue gas over IrO_2 modified Ce–Zr solid solution and the mechanism investigation

Wanmiao Chen, Zan Qu, Wenjun Huang, Xiaofang Hu, Naiqiang Yan *

School of Environmental Science and Engineering, Shanghai Jiao Tong University, Shanghai 200240, China

HIGHLIGHTS

- The $IrO_2/Ce_{0.6}Zr_{0.4}O_2$ (PVP) catalyst displayed excellent performance for NH_3 oxidation.
- SO_2 could inhibit the NH_3 removal, but also improved the N_2 selectivity to 100%.
- The mechanism of NH_3 oxidation follows two pathways at different temperature region.
- The internal SCR mechanism was the dominant reaction pathway over IrO_2 modified catalyst.

GRAPHICAL ABSTRACT

The mechanism of NH_3-SCO over $IrO_2/Ce_{0.6}Zr_{0.4}O_2$ (PVP) catalyst.

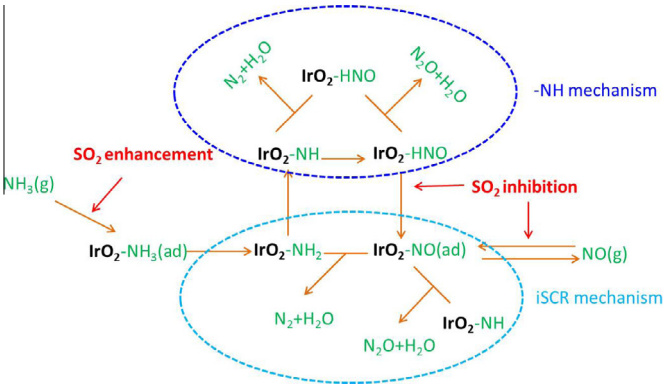

ARTICLE INFO

Article history:
Received 24 August 2015
Received in revised form 17 October 2015
Accepted 29 October 2015
Available online 2 November 2015

Keywords:
Slip ammonia
SCO
Ir
Internal SCR
DRIFT

ABSTRACT

The slip ammonia from selective catalytic reduction (SCR) of NO_x in coal-fired flue gas can cause degeneration of the utilities and environmental issues like aerosol. To achieve selective catalytic oxidation (SCO) of slip ammonia to N_2, novel IrO_2 modified Ce–Zr solid solution catalysts were synthesized and tested under various conditions. It was found that $IrO_2/Ce_{0.6}Zr_{0.4}O_2$ (PVP) catalyst displayed outstanding catalytic activity for slip ammonia and the removal efficiency was higher than 98%. Interestingly, the effect of SO_2 on NH_3 oxidation was bifacial, which the presence of SO_2 could result in slight deactivation of catalyst but also improve the N_2 selectivity of oxidized products to as high as 100% with coexistence of SO_2 and NH_3. The mechanism of NH_3-SCO process over $IrO_2/Ce_{0.6}Zr_{0.4}O_2$ (PVP) was evaluated through various techniques, and the results demonstrated that NH_3 oxidation could follow both —NH mechanism and internal SCR (iSCR) mechanism at different temperature regions. And the dominant pathway is the iSCR mechanism, in which adsorbed ammonia is firstly activated and reacts with oxygen atoms to form the —HNO intermediate. Then, the —HNO could be oxidized with atomic oxygen from O_2 to form NO species. Meanwhile, the formed/adsorbed NO could interact with —NH_2 to N_2 with N_2O as by-product, and the presence of SO_2 can effectively inhibit the production of N_2O and NO. Also, the mechanism of SO_2 effects was also evaluated and determined reasonably.

* Corresponding author. Tel./fax: +86 21 54745591.
E-mail address: nqyan@sjtu.edu.cn (N. Yan).

http://dx.doi.org/10.1016/j.fuel.2015.10.116
0016-2361/

1. Introduction

Nitrogen oxides (NO_x) which are mainly generated during the combustion process of fossil fuels, are one of major air pollutants from mobile and stationary pollution sources [1]. Selective catalytic reduction (SCR) of NO_x with NH_3 is considered as the most efficient and mature technology for reducing NO_x emission from coal-fired boiler flue gas. However, one drawback of this technology is that some amount of ammonia may pass through the system without reacted, especially for the aged catalysts, which is called ammonia slip. Because slip ammonia can cause a dust plug in the downstream air-preheater and even form secondary inorganic aerosols which contribute significantly to smog and haze after it is released into the atmosphere, it has been considered as a more sensitive air pollutant than NO_x [2]. In China, most coal-fired power plants are pursuing the so-called "ultra-low emissions standards", in which the emission NO_x concentration is limited to below 50 mg/m^3 or even less [3]. In such cases, higher NH_3/NO_x for SCR process will be employed and the slip ammonia will become a considerable issue. And the allowable concentration of ammonia slip for SCR system in coal-fired power plants has been tentatively regulated to less than 3 ppm in China [4] and suitable method must be found to eliminate this slippage. Meanwhile, the mercury emission from coal-fired power plants is also a worldwide concern, especially for China as the largest mercury emitting country [5]. To achieve slip ammonia and mercury removal simultaneously, the SCR-Plus catalyst over which the selective catalytic oxidation (SCO) to N_2 of ammonia and conversion of elemental mercury could proceed efficiently, has been proposed for installation at the tail-end of SCR units in our previous research [6]. In this way, not only does this catalyst reduce or eliminate ammonia slip and elemental mercury, but it can also lead to a better performance of an SCR catalyst by allowing a more aggressive dosing strategy to meet ultra-low emissions standards in China.

Many noble metals such as Au, Ru and Pt have been involved in the studies of selective catalytic oxidation of ammonia [7]. Ir has been employed as a catalyst for high concentration NH_3 oxidation in some previous researches [8], which indicates that IrO_2 has the potential to be the active component for SCR-Plus catalyst. However, IrO_2 catalyst has rarely been involved in coal-fired flue gas, and the effects of coal-derived flue gas which is a complex mixture (like SO_2, NO_x) on the IrO_2 modified catalysts have never been studied. What's more, the contents of Ir were very high in most researches, which is not acceptable for industrial application, therefore high efficient catalyst with low Ir concentration should be developed. Recently, ceria (Ce)–zirconia (Zr) solid solutions with cubic fluorite phases (Ce:Zr > 1:1), have served as catalyst carriers in many studies and drawn more attention due to their outstanding oxygen storage capacities and unique redox properties [9]. Moreover, Ce–Zr solid solution supported metal oxide catalysts exhibited excellent catalytic activity and N_2 selectivity for NO reduction via NH_3 [10]. Although the pathways of NH_3-SCO and NH_3-SCR are not identical, Ce–Zr solid solutions could be an attractive catalyst support for NH_3-SCO. In our previous research, we have found that Ce–Zr solid solutions supported catalysts displayed excellent activities for mercury removal [11], therefore, the main focus of this manuscript is the process of NH_3-SCO over IrO_2 modified Ce–Zr catalyst and mechanism research, especially the effects mechanism of SO_2 and NO_x as the most typical component in coal-fired flue gas. The catalytic activity and property of low concentration IrO_2 modified Ce–Zr catalysts for ammonia oxidation have never been studied and deserve to be determined.

Since Ir is usually considered as a noble metal and the price is more expensive than most of the transition metals (though the price of Ir is often about 50% that of Pt), the content of IrO_2 was set at very low level (0.2%). To maintain the catalytic performance of the catalyst while using lower Ir concentrations and make full use of it, sol–gel method with polyvinylpyrrolidone (PVP) was employed to enhance the dispersion of IrO_2 on catalyst surface. In this paper, the catalytic activity for slip ammonia and effect of representative components like SO_2 in coal-fired flue gas was tested at various conditions. N_2 is the perfect product for the NH_3-SCO process and few amount of NO and NO_2 is also acceptable. However, N_2O is undesirable due to its high greenhouse gas potential [12]. Therefore, the N_2 selectivity of the SCO products was also evaluated during the experiment. Although several studies have examined the NH_3-SCO process, the mechanism of NH_3 oxidation and N_2 formation is not clearly understood. Three major reaction pathways have been proposed for the SCO of NH_3 to N_2 over different catalysts [13,14]. However, the mechanism of NH_3-SCO over IrO_2 modified Ce–Zr complex has not been studied in detail. To rationally develop the process of NH_3 oxidation to N_2 over IrO_2 modified catalysts for slip ammonia for coal-fired flue gas, the effect of components in coal-fired flue gas like SO_2 and the reaction mechanism must be clarified. Temperature programmed oxidation (TPO), temperature-programmed desorption (TPD) and in situ diffuse reflectance infrared Fourier transform spectroscopy (DRIFT) were used to determine the possible reaction mechanisms.

2. Experimental section

2.1. Materials and catalyst preparation

The IrO_2 modified catalysts were synthesized according to method from literature [15]. Polyvinylpyrrolidone (PVP, Mw = 58,000) and quantitative Iridium acetate was dissolved in 30 ml of ethanol. The mixture was refluxed at 100 °C for 3 h to make the Ir gel. Next, the Ir colloidal solution was added to $Ce_xZr_{1-x}O_2$ (Appendix), and the mixture was dried at 60 °C for evaporation with electromagnetic stirring. Then, the catalysts were calcined at 400 °C for 5 h in air with a 1 °C/min ramping rate from room temperature and labeled as $IrO_2/Ce_xZr_{1-x}O_2$ (PVP). The $IrO_2/Ce_xZ_{1-x}O_2$ catalyst was prepared using the normal wet impregnation method. The IrO_2 content of $Ce_xZr_{1-x}O_2$ was set at 0.2 wt.% for all catalysts. All chemicals used for the preparation of catalysts were of analytical grade and were purchased from Sigma–Aldrich Co. or Sino-pharm Chemical Reagent Co. The SO_2, NH_3 and NO gases were supplied by Weichuan Gas Co.

2.2. Catalytic activity measurement

The performance of the catalysts for NH_3 oxidation was tested in a fixed-bed quartz reactor. The catalyst particles were placed in the reactor with quartz wool under atmospheric pressure and was heated using a vertical electrical furnace. The gases consisting of NO_x, NH_3, 4% O_2, SO_2 (if need) in N_2 were adjusted by mass flow controllers and introduced into the reactor with a total flow rate of 500 ml/min. The concentrations of SO_2, NH_3, NO, NO_2 and N_2O were continually monitored with FTIR Multigas analyzer (IMACC, E-3200-C). The NH_3-TPO was performed out from 50 °C to 400 °C with a 1 °C/min ramping rate. The NH_3 removal efficiency and N_2 selectivity was calculated using Eqs. (1) and (2) as follow:

$$\text{NH}_3\text{ removal efficiency} = \frac{[\text{NH}_3]_{\text{inlet}} - [\text{NH}_3]_{\text{outlet}}}{[\text{NH}_3]_{\text{inlet}}} \times 100\% \quad (1)$$

$$\text{N}_2\text{ selectivity} = \left[1 - \frac{[\text{NO}]_{\text{outlet}} + [\text{NO}_2]_{\text{outlet}} + 2[\text{N}_2\text{O}]_{\text{outlet}}}{[\text{NH}_3]_{\text{inlet}} - [\text{NH}_3]_{\text{outlet}}}\right] \times 100\% \quad (2)$$

2.3. NH_3-TPD

The NH_3-TPD curves were collected using chemisorption analyzer (2920, AutoChem II, Micromeritics). Prior to the measurement, the samples were first treated in a He stream at 350 °C to remove physically adsorbed matter. NH_3 adsorption was then performed at 100 °C with 10% NH_3 for 1 h. Next, the samples were purged in He stream for 30 min to remove physically adsorbed NH_3, and then heated to 600 °C with temperature ramp of 10 °C/min with a 50 sccm He flow. Desorbed NH_3 was detected with a thermal conductivity detector (TCD).

2.4. In situ DRIFT Studies

In situ DRIFT spectra were recorded on a Fourier transform infrared spectrometer (FTIR, Nicolet 6700) equipped with a smart collector and an MCT detector cooled by liquid N_2. The diffuse reflectance FTIR measurements were carried out in a high-temperature cell with ZnSe windows. Mass flow controllers and a sample temperature controller were used to simulate the real reaction conditions. Prior to each experiment, the catalyst was heated to 400 °C in N_2 with a total flow rate of 250 ml/min for 3 h. The IR spectra were recorded by accumulating 100 scans at a resolution of 4 cm^{-1}.

3. Results and discussion

3.1. Catalytic activity

NH_3-TPO experiments were performed separately over three catalysts to evaluate the NH_3 oxidation activity and N_2 selectivity over $Ce_{0.6}Zr_{0.4}O_2$, $IrO_2/Ce_{0.6}Zr_{0.4}O_2$ and $IrO_2/Ce_{0.6}Zr_{0.4}O_2$ (PVP) catalysts and the results were shown in Fig. 1 (preliminary experiments at 350 °C (Fig. A1) showed that $Ce_{0.6}Zr_{0.4}O_2$ supported catalysts displayed superior catalytic activity). The results displayed that NH_3 could not be oxidized and no products were formed until the temperature was above 300 °C over $Ce_{0.6}Zr_{0.4}O_2$ and the oxidation efficiency of ammonia was only about 40% even the temperature increased to 400 °C, which meant that the $Ce_{0.6}Zr_{0.4}O_2$ had poor catalytic activity for NH_3-SCO reaction. While, the initial reaction temperature decreased to approximately 160 °C when only 0.2% IrO_2 adding to $Ce_{0.6}Zr_{0.4}O_2$ catalyst, which indicated that doping with IrO_2 could facilitate NH_3 oxidation at lower temperature. Also, the NH_3 oxidation efficiency at 400 °C over $IrO_2/Ce_{0.6}Zr_{0.4}O_2$ increased to 87%. Meanwhile, the synthetic method could also have an effect on the catalytic activity and almost 99% NH_3 were oxidized over $IrO_2/C_{0.6}Z_{0.4}O_2$ (PVP) when temperature increased to 400 °C. We propose that PVP might promote IrO_2 dispersion over carrier just similar in other researches and result in superior catalytic activity [15].

In addition, the NH_3 oxidation products over various catalysts were also determined during the TPO experiment. The main detectable product was NO over $Ce_{0.6}Zr_{0.4}O_2$ and the N_2 selectivity was over 75%. And very little amount of N_2O (lower than 1 ppm) was also detected in oxidation products simultaneously with NO. However, the N_2 selectivity was only approximately 60% for $IrO_2/Ce_{0.6}Zr_{0.4}O_2$. In addition, more NO was generated during the process of NH_3 oxidation over PVP promoted $IrO_2/Ce_{0.6}Zr_{0.4}O_2$ catalysts, and the N_2 selectivity was approximately 15% lower than normal $IrO_2/Ce_{0.6}Zr_{0.4}O_2$. It seems that N_2 selectivity decreased with catalytic activity was enhanced. Also, it could be noticed that N_2O was first generated over $IrO_2/Ce_{0.6}Zr_{0.4}O_2$ and $IrO_2/Ce_{0.6}Zr_{0.4}O_2$ (PVP) catalysts at about 160 °C when the ammonia started to be oxidized. And NO was formed until the temperature was over 200 °C, while NO and N_2O were detected at same temperature over $Ce_{0.6}Zr_{0.4}O_2$ catalysts. According to some literature reports, NH_3 could be oxidized at lower temperatures (around 150 °C) over some catalysts (especially Ag-modified catalysts), and N_2O was the main product [13]. Two disparate reaction pathways, for high and low temperatures, respectively, were proposed to explain this situation. Similar phenomena was observed over the $IrO_2/Ce_{0.6}Zr_{0.4}O_2$ catalyst, which indicated that the doping of IrO_2 could make the low temperature reaction pathway feasible and there might be two possible mechanisms for NH_3-SCO in our research for low and high temperatures.

Also, the effects of common components in coal-fired flue gas on NH_3-SCO over IrO_2 modified catalysts were evaluated and the results are shown in Fig. 2. Firstly, the gas with approximately 30 ppm NH_3 was switched to the $IrO_2/Ce_{0.6}Zr_{0.4}O_2$ (PVP) in the

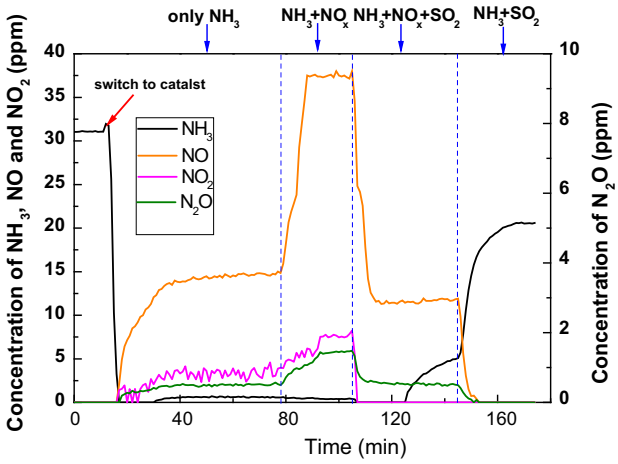

Fig. 2. The effect of NO_x and SO_2 on NH_3-SCO at 350 °C over $IrO_2/Ce_{0.6}Zr_{0.4}O_2$ (PVP). The space velocity (SV) was approximately 3.8×10^5 h^{-1}. The temperature was 623 K. 30 ppm NH_3, 30 ppm NO and 500 ppm SO_2. The other gas compositions were 4% O_2 and N_2.

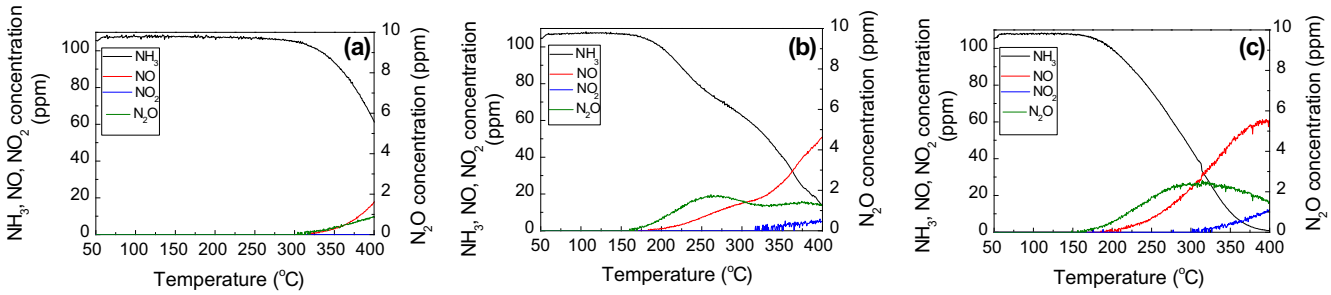

Fig. 1. The NH_3-TPO profiles of $Ce_{0.6}Zr_{0.4}O_2$ (a), $IrO_2/Ce_{0.6}Zr_{0.4}O_2$ (b) and $IrO_2/Ce_{0.6}Zr_{0.4}O_2$ (PVP) (c) catalysts. Reaction conditions: NH_3 110 ppm; O_2, 4 vol.%; N_2 as carrier; flow rate, 500 ml/min; catalyst weight, 60 mg. The space velocity (SV) was approximately 3.8×10^5 h^{-1}.

reaction tube after the NH_3 concentration was stable. Because of the adsorption over the catalyst, no ammonia was detected in the exhaust at the initial stage. However, some amount of NO, NO_2 and N_2O could be detected very soon after the NH_3 was introduced to the reaction tube, which meant that the ammonia could be oxidized as soon as contacting the catalyst. After the adsorption equilibration was reached, about 0.7 ppm NH_3 could be detected in the exhaust, corresponding to 98% oxidation efficiency. While, the N_2 selectivity of the oxidation products was only about 40% since about 14 ppm NO was formed. Fortunately, the generated N_2O concentration was only 0.5 ppm which was acceptable level. Since the catalysts are proposed to be installed at the tail of SCR unit, NO_x would exist in flue gas during operation. Therefore, the NH_3 oxidation efficiency in the presence of NO_x over catalyst was also evaluated. After about 30 ppm NO_x was added into the gas, the concentration of NH_3 decreased to 0.38 ppm, which indicated that NO_x could promote NH_3 removal. It might be explained as NH_3 being oxidized through the SCR pathway in the presence of NO_x (Reactions (1) and (2)), which indicates that the catalysts also have the potential for De-NO_x.

$$4NH_3 + 6NO \rightarrow 5N_2 + 6H_2O \quad (1)$$

$$8NH_3 + 6NO_2 \rightarrow 7N_2 + 12H_2O \quad (2)$$

Usually, SO_2 in coal-fired flue gas would have deactivation on catalysts. However, the effect of SO_2 on NH_3 oxidation is very different in this study. With the presence of NO_x, SO_2 could slightly promote the NH_3 removal efficiency to 100% at the initial stage and then the removal efficiency of NH_3 gradually decreased to about 85% until equilibrium. Meanwhile, the adding of 500 ppm SO_2 could also decrease the concentration of NO, NO_2 and N_2O and the NO_2 could not even be detected, which meant that SO_2 could benefit N_2 selectivity to 100% and it was perfect result for NH_3 oxidation. While similar effect occurred when only NH_3 and SO_2 existed in the gas. After the NO_x was suspended, the NH_3 oxidation efficiency dropped significantly to only 35%. What's more, no NO_x was detected in the exhaust, which meant the N_2 selectivity increased to 100% by the SO_2. Therefore, the effect of SO_2 on NH_3 oxidation was bifacial, which had rarely been reported in other researches. SO_2 could facilitate the NH_3-SCO at first initial stage with the coexistence of NO_x, and inhibit NH_3 removal afterward. And SO_2 could also improve the N_2 selectivity of NH_3 oxidation products to 100%.

3.2. DRIFT of NH_3 adsorption

To determine the mechanism of SO_2 effects on NH_3-SCO, the reaction pathway of NH_3 oxidation over the catalyst should be clarified in first place. Therefore, the in-situ DRIFT was employed to evaluate the possible mechanism of NH_3 oxidation. Firstly, DRIFT spectra of NH_3 adsorption over $IrO_2/Ce_{0.6}Zr_{0.4}O_2$ (PVP) catalyst at different temperatures are showed in Fig. 3. As shown in figure, several bands at 1105, 1151, 1299, 1415, 1589 cm^{-1} were observed after the catalyst sample was pre-treated under 500 ppm NH_3 at 50 °C. The bands centered at 1589 and 1105 cm^{-1} could be assigned to asymmetric and symmetric deformation of coordinated ammonia on Lewis sites, respectively [16,17]. The bands at 1299 and 1151 cm^{-1} can also be assigned to the symmetric deformation of ammonia coordinately bonded to one type of Lewis acid sites [18]. The weak band at 1415 cm^{-1} was ascribed to the asymmetric bending vibrations of ammonium ions chemisorbed of adsorbed on Brønsted sites [18,19]. The negative band at 1630 cm^{-1} was ascribed to O—H stretching vibration modes due to the interaction of surface hydroxyls with NH_3 [20]. In the NH stretching region, bands were found at 3159, and 3373 cm^{-1}, together with negative bands at 3689 and 3658 cm^{-1} due to the hydroxyl consumption through interaction with NH_3 to form NH_4^+ [13]. While, the band at 3257 was assigned to the coordinated NH_3 [21]. The intensity of the 1415 cm^{-1} band assigned to Brønsted acid sites decreased noticeably with the increasing temperature, and vanished at 200 °C. Also, the band at 1105 cm^{-1} disappeared when the temperature increased to 100 °C. In addition, the intensity of the band at 1589 cm^{-1} also weakened as the temperature increased and disappeared at 200 °C. And the bands at 1299 cm^{-1} shifted to 1270 cm^{-1} as the temperature increased and vanished at 250 °C. What's more, the peak at 1151 cm^{-1}, due to Lewis acid sites, weakened and shifted to 1170 cm^{-1} as the temperature increased and the peak could be detected until 350 °C. As shown in results, the intensity of the bands ascribed to coordinately bonded ammonia to Lewis acid sites were much stronger than that on Brønsted sites, which meant the adsorbed ammonia mainly existed in form of coordinately bonded ammonia rather than NH_4^+. What's more, the bands due to Lewis acid sites still remained at 300 °C, which indicated that ammonia bonded to Lewis acid sites were more stable.

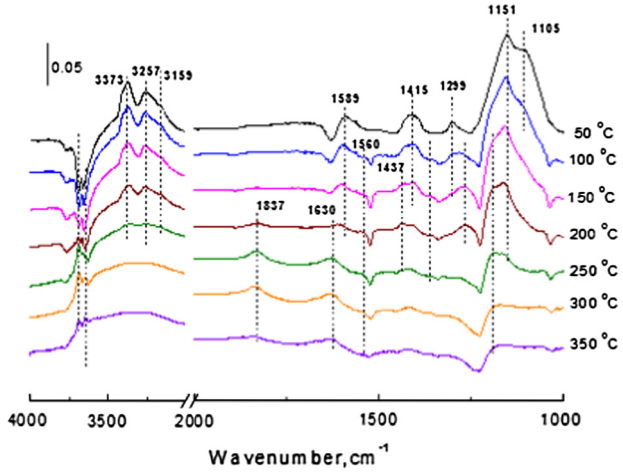

Fig. 3. DRIFT of $IrO_2/Ce_{0.6}Zr_{0.4}O_2$ (PVP) treated with NH_3 at 50 °C and successive purging with N_2 at various temperature.

Another weak band at 1059 cm^{-1} could be observed during heating under N_2, and the band might be caused by ammonia hydrogen bonding to the surface oxygen atoms of cerium oxide accordingly [22]. Three new weak bands at 1365, 1437, 1560 cm^{-1} could be detected over the catalyst when the temperature increased to 100 °C, which belonged to neither Lewis nor Brønsted acid sites. According to some literatures, the bands at 1365 and 1560 cm^{-1} were assigned amide (—NH_2) wagging and scissoring, respectively [13,17]. While, the band at 1437 cm^{-1} might be ascribed to —NH deformation models, another intermediate of the ammonia oxidation [13,23,24]. Two new bands at 1837 and 1630 cm^{-1} appeared as the temperature increased to 200 and 250 °C, respectively. The band at 1832 cm^{-1} was assigned to nitrosyl (—HNO) formed over the catalyst [25] and the band centered at 1630 cm^{-1} was due to nitrate species [26]. These results indicated that, upon heating the adsorbed NH_3 would be activated to form —NH_2 and —NH intermediates through the abstraction of hydrogen. While, the intensity of bands ascribed to —NH_2 (1365 and 1560 cm^{-1}) and —NH (1437 cm^{-1}) were very weak, perhaps because the intermediates reacted quickly with oxygen atoms from the Ce–Zr solid solution, which has an outstanding oxygen storage capacity. This could also explain that bands due to nitrosyl and adsorbed nitrate species showed up at as temperature increased.

$$NH_3 \rightarrow NH_2 + H \quad (3)$$

$$NH_2 \rightarrow NH + H \quad (4)$$

$$NH + O \rightarrow HNO \quad (5)$$

3.3. The interaction of NH_3 with O_2

The behavior of adsorbed NH_3 species interacting with O_2 in gas over $IrO_2/Ce_{0.6}Zr_{0.4}O_2$ (PVP) catalyst was evaluated through in situ DRIFT spectra (Fig. 4(a)) and the spectra of 150–200 °C was also given in Appendix to provide more details (Fig. A2). The bands of NH_3 assigned to Brønsted acid sites (1413 cm^{-1}) and Lewis acid sites (1108, 1153, 1298 and 1590 cm^{-1}) decreased gradually and disappeared at temperatures above 200 °C. When the intensity of these bands decreased, a weak new band at 1438 cm^{-1}, assigned to —NH, appeared at 100 °C, which agrees with the results in Fig. 3. A new peak at 1626 cm^{-1} appeared at 170 °C, which was attributed to bridging nitrate (nitrate species) [21], and the band of —NH at 1438 cm^{-1} and —NH_2 at 1365 decreased as the temperature increased to 200 °C. Another band at 1700 cm^{-1} also appeared over the catalyst when the temperature increased to 190 °C and it indicated the oxidation of ammonia into acylamide species with the presence of O_2, which acylamide structure had been proposed to be intermediates of the SCR [21]. As the temperature increased to 190 °C, four new peaks at 1524, 1221 and 1031, 1013 cm^{-1} showed up, and they were assigned to adsorbed nitrate species (1524 for monodentate nitrate, 1221 for bridging nitrate, 1031 for bidentate nitrate and 1013 for *cis*-$N_2O_2^{2-}$) [17,26,27]. All these results indicated that the adsorbed ammonia started to be oxidized to N_2 and NO with O_2 at temperature of approximately 190 °C over the $IrO_2/Ce_{0.6}Zr_{0.4}O_2$ (PVP) catalyst, which was in agreement with the temperature in TPO result that NO was detected at about 190 °C. In our previous research, the intensity of all the bands over catalysts decreased noticeably upon heating to 350 °C, due to the desorption of the produced/adsorbed NO species at higher temperatures [11]. However, in this research, the intensity of all of the bands attributed to nitrate species remained unchanged, which indicated the bonding between nitrate species and the IrO_2 modified catalyst was much stronger.

A new weak band at 2218 cm^{-1} was observed and enhanced from 190 °C to 300 °C, which weakened as at temperature above 300 °C. Similar bands at 2222 and 2200 cm^{-1} upon NH_3 oxidation on carbon [28] and ZnO [13] catalysts had been ascribed to N—N stretching modes of adsorbed N_2O. Accordingly, the appearance of more than one form of adsorbed N_2O is often explained by the simultaneous presence of N— and O— bonded molecules. When the N—O modes of adsorbed N_2O were detected, they were registered in the region of 1262–1220 cm^{-1} [29]. Interestingly, a weak band at 1252 cm^{-1} was detected indeed, and it appeared at 170 °C and decreased at temperature above 300 °C, just like the band at 2218 cm^{-1}. So it could be concluded that the bands at 1252 cm^{-1} and 2218 cm^{-1} were assigned to adsorbed N_2O from the oxidation of ammonia, which was consistent with TPO results.

In situ DRIFT spectra of O_2 passing over an NH_3-pretreated catalyst at 350 °C were also recorded and are shown in Fig. 4(b). After the catalyst was treated with 500 ppm NH_3 and purged with N_2, though some adsorbed ammonia species desorbed under N_2 purging, bands ascribed to ammonia species linked to Brønsted sites (1414 cm^{-1}) and Lewis sites (1060, 1147) and were observed. And also the bands due to the amide (—NH_2) at 1312 cm^{-1}, which is intermediate of the reaction. As shown in Fig. 4(b), the bands attributable to the produced nitrate species (1524, 1221, 1031 cm^{-1}) were observed after 4% O_2 was introduced for 3 min and the bands for adsorbed ammonia all disappeared in 5 min, which meant that the adsorbed NH_3 species could be oxidized quickly by O_2.

3.4. The interaction of NH_3 with formed nitrate species

The interaction of gaseous NH_3 with in situ formed nitrate species over the catalyst was also investigated to evaluate the reaction

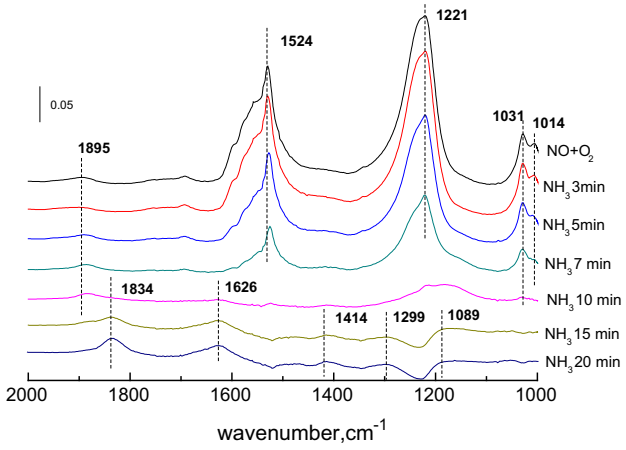

Fig. 5. Interaction of NH_3 with formed NO species on $IrO_2/Ce_{0.6}Zr_{0.4}O_2$ (PVP) catalyst at 350 °C.

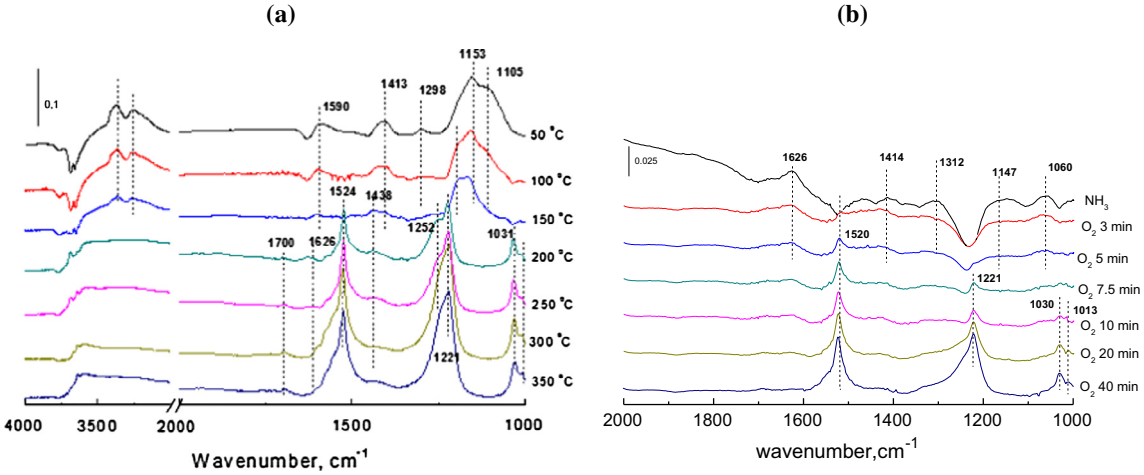

Fig. 4. (a) DRIFT of $IrO_2/Ce_{0.6}Zr_{0.4}O_2$ (PVP) treated with NH_3 at 50 °C and successive purging with 4% O_2 at various temperature and (b) interaction of O_2 with formed NH_3 on $IrO_2/Ce_{0.6}Zr_{0.4}O_2$ (PVP) catalyst at 350 °C.

mechanism. Firstly, the catalyst was exposed to gas with 500 ppm NO_x and 4% O_2 at 350 °C until the saturated adsorption of NO_x. Then, the sample was purged with N_2 for 30 min to remove physically adsorbed NO_x. After that, 200 ppm NH_3 with N_2 carrier was introduced and in-situ DRIFT spectra were recorded. The results are shown in Fig. 5. Several bands ascribed to adsorbed nitrate species at 1524, 1221, 1031 and 1014 cm^{-1} were observed after the NO and O_2 passed over the catalysts for a brief time. Following NH_3 inflow for 3 min, the bands due to nitrate species began to decrease, which indicated gaseous NH_3 could be adsorbed to the surface first and then reacted with nitrate species species quickly. The bands assignable to adsorbed NH_3 species (1414, 1147 and 1060 cm^{-1}) appeared on the catalyst following the NH_3 flow in 10 min, and the intensity increased with the exposure time. And we could notice that the intensity of the bands to nitrate species were much stronger than that of adsorbed ammonia, which meant NO_x were much more easily be adsorbed to the surface of the IrO_2 modified catalysts than NH_3.

The shifting of band at 1895 cm^{-1} could be observed during the experiment. The band at 1895 cm^{-1} shifted to 1881 cm^{-1} following the NH_3 inflow in 10 min, and eventually be detected at 1833 cm^{-1}. Accordingly, some studies proposed that the bands around at region of 1890–1830 cm^{-1} may relate to the produced/adsorbed NO [30,31]. However, this is not applicable for all situations in our research, since similar band during NH_3 adsorption (Fig. A3) when no NO_x existed. A similar shifting of the band was also observed in our previous research and the bands at adjacent region were identified to different species [11]. According to some literature reports, the band at 1834 cm^{-1} is in the typical range of symmetric stretching vibration of dinitrosyl (nitrosyl in double) [32]. To identify the band, firstly, the spectrum of NH_3 and NO adsorption over $Ce_{0.6}Zr_{0.4}O_2$ were recorded, and no identical peak appeared on the surface of $Ce_{0.6}Zr_{0.4}O_2$ in both NH_3 and NO DRIFT adsorption spectra (Fig. A4). Clearly, it can be concluded that the bands in the range of 1900–1800 cm^{-1} are related to the Ir species in the catalyst. When the NH_3 passed over the NO pretreated catalyst, the band gradually shifted from 1895 cm^{-1} to 1834 cm^{-1}. And the band at 1834 cm^{-1} could be detected when the catalyst was exposed under NH_3 (Fig. A3). Therefore, it is reasonable to assign the band at 1834 cm^{-1} to nitrosyl formed from via the dehydrogenation of NH_3 adsorbed to IrO_2, which was so weak on the catalyst that to be detected after N_2 purging. And 1895 cm^{-1} is assigned to adsorbed NO species linked to IrO_2.

Synthesizes the results of TPO and DRIFT spectra above, the oxidation of NH_3 over the $IrO_2/Ce_{0.6}Zr_{0.4}O_2$ (PVP) catalyst follows two different pathways simultaneously. At relatively low temperature region (160–300 °C, in the region N_2O was formed at 160 °C and began to decrease at 300 °C as shown in TPO results), the oxidation of ammonia could take place through the —NH mechanism. The intermediate of —NH was firstly oxidized to HNO by the oxygen atom from the dissociation of O_2. Then the HNO could react itself to form N_2O Reaction ((6)).

$$HNO + HNO \rightarrow N_2O + H_2O \quad (6)$$

Since the concentration of produced N_2O was very low, this mechanism should not be the main pathway of ammonia oxidation, especially at temperature above 300 °C. While, at temperature above 190 °C which the generated NO was first detected in exhaust, the oxidation of ammonia follows an internal SCR (iSCR) mechanism. It began with dehydrogenation and oxidation of NH_3 into NO species Reactions ((3–5), (7 and 8)), followed by formed/adsorbed NO species interacting with amide and being reduced to N_2 with N_2O as by-product Reactions ((9)–(11)). The formed —NH_2 or —NH and NO species are the intermediates in this reaction pathway. The overall reaction for SCO-NH_3 is Reaction (12).

$$O_2 \rightarrow 2O \quad (7)$$

$$HNO + O \rightarrow NO + OH \quad (8)$$

$$NH_2 + NO \rightarrow N_2 + H_2O \quad (9)$$

$$NH + NO \rightarrow N_2O + H \quad (10)$$

$$H + OH \rightarrow H_2O \quad (11)$$

$$4NH_3 + 3O_2 \rightarrow 2N_2 + 6H_2O \quad (12)$$

3.5. DRIFT of SO_2 adsorption

Since the effect of SO_2 on NH_3 removal over the catalysts was bifacial as shown in Fig. 2, the mechanism of the SO_2 effect was also investigated through DRIFT spectra. The in-situ DRIFT spectrum of 500 ppm $SO_2 + O_2$ interacting with $IrO_2/Ce_{0.6}O_{0.4}O_2$ (PVP) catalyst at 350 °C was recorded and shown in Fig. A5. After exposing to $SO_2 + O_2$ for 60 min, several bands at 1630, 1378, 1161, 1060 and 993 cm^{-1} were observed on the catalyst. The bands at 1060 and 997 cm^{-1} were assignable to the stretching motion of adsorbed "inorganic" sulfate on the surface, which were the triply degenerate asymmetric stretching $v3$ band of the bidentate sulfate complex and nondegenerate symmetric stretching $v1$ band, respectively [33]. The band at 1378 cm^{-1} was attributed to the asymmetric vibration modes of O═S═O ($\nu_{as\ S=O}$), which was a typical "organic" sulfate species with covalent S═O double bonds [34]. Additionally, the strongest band at 1161 cm^{-1} was attributed to abundant sulfate species [35]. The negative peak at 3656 cm^{-1} was attributed to the interaction of SO_2 with surface hydroxyl groups, which might induce change in the OH stretching vibration resulting from the formation of hydrogen-bonded sulfite species [36]. It is also could be inferred that surface-bonded water was formed since the band assigned to δ_{HOH} of H_2O at 1631 cm^{-1} and a broadband in the region of 3500–3100 cm^{-1} in the spectra simultaneously appeared over the spectra [35].

3.6. Adsorption of NH_3 and NO on sulfated catalyst

As we know, adsorption of reactants on the catalyst surface was very crucial to the catalytic reaction, to determine the effect mechanism of SO_2 on ammonia oxidation, the effects of SO_2 on adsorption for NH_3 and NO were tested firstly. The profiles of the NH_3-TPD analysis of catalysts are given in Appendix (Fig. A6). One major desorption peak was observed with the $Ce_{0.6}Zr_{0.4}O_2$ catalyst at 200 °C, which might be attributed to ammonia weakly adsorbed on acid sites including Lewis and Brønsted acids. After doping with IrO_2, the main peak at 200 °C was much weaker, and a board shoulder starting at 250 °C was observed over $IrO_2/Ce_{0.6}Zr_{0.4}O_2$, which indicated that the adsorption ability for NH_3 of catalyst was weakened by doping of IrO_2. Although less NH_3 was adsorbed to $IrO_2/Ce_{0.6}Zr_{0.4}O_2$ catalyst, it displayed a superior NH_3 oxidation efficiency due to the excellent catalytic activity of IrO_2. The profile of the sulfated catalyst was much different. The board shoulder started at 150 °C and increased gradually alone with temperature rising. Another desorption peak could be detected at about 450 °C. Less NH_3 desorbed from the sulfated catalyst at lower temperatures (<300 °C) than that of higher temperatures, which meant sulfation by SO_2 could strengthen the bonding between NH_3 and the catalysts and enhance the NH_3 adsorption at higher temperatures. What's more, the DRIFT spectra of ammonia adsorption on fresh and sulfated catalysts were also given (Fig. A7). As shown in results, the intensity of the bands due to adsorbed ammonia species on the fresh catalyst was much weaker than that on sulfated catalyst at 350 °C, which also indicated that SO_2 could improve the adsorption of ammonia on the catalyst.

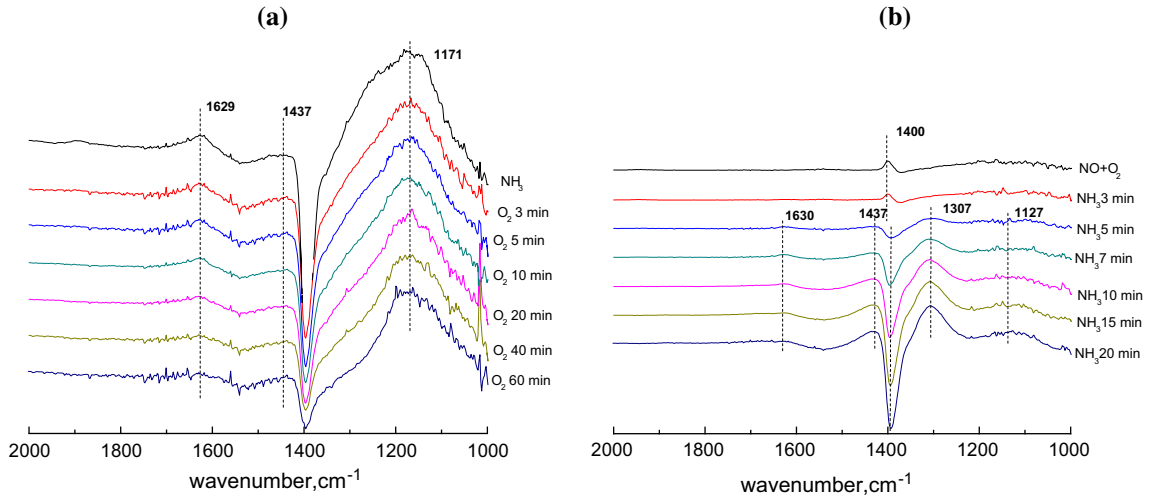

Fig. 6. (a) Interaction of O_2 with formed NH_3 and (b) interaction of NH_3 with formed NO species on sulfated $IrO_2/Ce_{0.6}Zr_{0.4}O_2$ (PVP) catalyst at 350 °C.

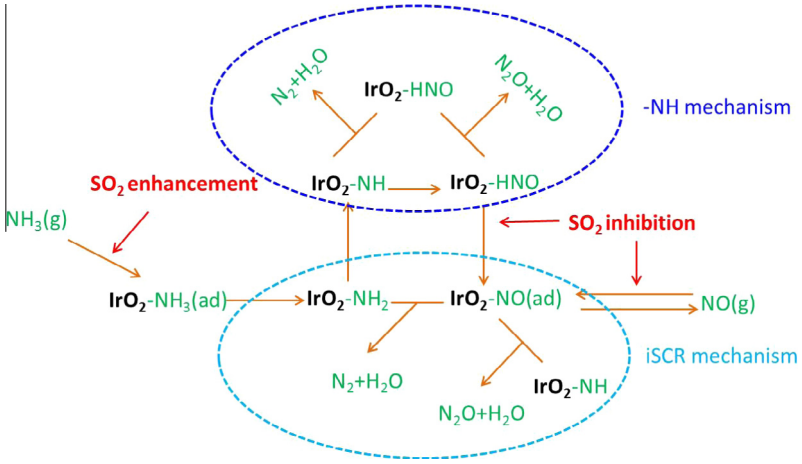

Fig. 7. The mechanism of NH_3-SCO over $IrO_2/Ce_{0.6}Zr_{0.4}O_2$ (PVP) catalyst.

Additionally, the DRIFT spectra of NO adsorption on fresh and sulfated catalysts were also recorded at 350 °C (Fig. A8). Unlike NH_3 adsorption, the intensity of bands assigned to nitrate species on fresh catalyst was very strong and the max absorbancy was about 0.25. While, the bands ascribed to nitrate species on SO_2 pretreated catalyst were much lower and the max absorbancy was only about 0.018. Therefore, it could be concluded that SO_2 could slightly enhance the adsorption of ammonia, but could also inhibit the NO adsorption over the catalyst significantly.

3.7. DRIFT spectra of reaction on sulfated catalysts

The interaction of NH_3 and NO_x on sulfated catalysts was also tested through DRIFT to determine the effect mechanism effects. Firstly, sulfated $IrO_2/Ce_{0.6}Zr_{0.4}O_2$ (PVP) catalyst was pretreated with NH_3 and N_2 purging, and then 4% O_2 was introduced to pass over the catalyst. After the adsorption of NH_3 on the sulfated catalyst at 350 °C, bands at 1171, 1437 and 1629 cm^{-1} were observed on the surface of the catalyst (Fig. 6(a)). After the O_2 passed through the sulfated $IrO_2/Ce_{0.6}Zr_{0.4}O_2$ (PVP) catalyst, the intensity of the bands assigned to adsorbed NH_3 species decreased very slowly. After interaction with 4% O_2 for 60 min, no obvious bands assigned to nitrate species were observed over the catalysts. Therefore, it is rational to conclude that the oxidation of —NH_2 to NO species (Reaction (8)) was severely inhibited after the sulfation of $IrO_2/Ce_{0.6}Zr_{0.4}O_2$ (PVP) catalyst.

The interaction of NH_3 with formed/adsorbed NO was also performed over sulfated catalyst and the DRIFT spectra are shown in Fig. 6(b). As mentioned above, the adsorption of NO was seriously suppressed by SO_2, so only very weak band at 1400 cm^{-1} was detected on the catalyst surface. After interacting with NH_3 for 5 min, the band ascribed to NO species vanished and new bands at 1127, 1307, 1437 and 1630 cm^{-1}, which were assigned to adsorbed NH_3 species, were detected on the spectra. This result meant that adsorbed/formed NO could still react with NH_3 on the sulfated catalyst through Reactions (9) and (10).

3.8. The mechanism of SO_2 effect

It has been proposed in the previous section that the selective catalytic oxidation of NH_3 over IrO_2 modified $Ce_{0.6}Zr_{0.4}O_2$ catalyst mainly followed the iSCR mechanism (Fig. 7). When SO_2 was present, gaseous ammonia was more easily adsorbed to the surface of catalyst due to the increase of the acid sites from sulfation, which explain the results in Fig. 2 that the removal efficiency of NH_3 increased at the initial stage of adding SO_2 into the gas. Then, more —NH_2 would be generated on the surface of the catalyst as the concentration of adsorbed NH_3 increased. As mentioned above,

the oxidation process of —NH_2 to NO species was seriously inhibited on the sulfated catalysts. What's more, the adsorption of NO species from gaseous phase on the catalyst was also suppressed by the presence of SO_2. In this way, the concentration of NO species on the surface, which was important intermediate of the reaction, decreased significantly even though with the existence of NO because both of the two sources of NO species were restrained by the presence of SO_2. Even though Reactions (9) and (10) could still proceed over sulfated catalyst, the consumption rate of —NH_2 on the catalyst through Reactions (9) and (10) was restricted because less NO species was formed (neither generated from oxidation of —NH_2 nor adsorbed from gaseous phase). Therefore, once the saturation of the NH_3 adsorption caused by the sulfation was reached, the NH_3 removal efficiency started to reduce just like the result in Fig. 2.

The situation would be similar in the absence of NO. The results of in situ DRIFT (Fig. 6) demonstrated that Reaction (8) was severely inhibited over the sulfated catalyst. Therefore, the NH_3 oxidation efficiencies over sulfated catalysts were lower than those over fresh catalysts in the absence of NO_x because there are fewer intermediates: NO was formed. Meantime, the concentration of —NH_2 on the catalyst increased as stated above. Therefore, the consumption of generated NO over the sulfated catalyst will be much quicker than over a fresh catalyst, since more —NH_2 was generated through adsorption and Reactions (9) and (10) could still proceed over the sulfated catalyst. Because less NO was generated and consumed completely (through Reactions (9) and (10)) at once, none of formed NO could be released into the gaseous phase, which explained the result that no NO_x was detected and the N_2 selectivity was as high as 100% with only NH_3 and SO_2.

4. Conclusion

In conclusion, the PVP promoted 0.2% IrO_2-modified $Ce_{0.6}Zr_{0.4}O_2$ catalyst displayed excellent catalytic performance for the selective catalytic oxidation of slip ammonia with various conditions. SO_2 can enhance the removal of slip ammonia at initial stage and inhibit the NH_3-SCO subsequently, but also significantly improved the N_2 selectivity to 100%. The pathway of slip ammonia oxidation over the $IrO_2/Ce_{0.6}Zr_{0.4}O_2$ catalyst could follow two different mechanisms. At lower temperature, ammonia oxidation could marginally react through —NH mechanism, in which the formed HNO reacts with itself to N_2O as by product. The dominant mechanism of ammonia oxidation over $IrO_2/Ce_{0.6}Zr_{0.4}O_2$ follows iSCR mechanism. Adsorbed ammonia is first activated and dehydrogenates with oxygen atoms to form HNO intermediate. Then, the HNO mainly reacts with atomic oxygen from O_2 to form adsorbed NO species. Finally, formed/adsorbed NO interacts with —NH_2 to N_2 with N_2O as a by-product. The presence of SO_2 could inhibit the process of the oxidation from formed HNO to NO species, but has negligible effect on interaction of formed/adsorbed NO with —NH_2 intermediate.

Acknowledgments

This study was supported by the National Basic Research Program of China (973) under Grant No. 2013CB430005, the NSFC projects (21277088, 21077073).

Appendix A. Supplementary material

Supplementary data associated with this article can be found, in the online version, at http://dx.doi.org/10.1016/j.fuel.2015.10.116.

References

[1] Bare J. TRACI 2.0: the tool for the reduction and assessment of chemical and other environmental impacts 2.0. Clean Technol Environ Policy 2011;13:687–96.
[2] Wen L, Chen J, Yang L, Wang X, Xu C, Sui X, et al. Enhanced formation of fine particulate nitrate at a rural site on the North China Plain in summer: the important roles of ammonia and ozone. Atmos Environ 2015;101:294–302.
[3] Mepc A. Emission standard of air pollutants for thermal power plants, GB13223-2011. Beijing: China Environmental Science Press; 2011.
[4] Engineering technical specification of flue gas selective catalytic reduction denitration for thermal power plant. HJ 562-2010; 2010.
[5] Wang H, Ma Z, Lu P, Cao Y, Pan W-P. Modeling of mercury speciation and capture in coal-fired flue gas. In: Cleaner combustion and sustainable world. Springer; 2013. p. 515–9.
[6] Chen W, Ma Y, Yan N, Qu Z, Yang S, Xie J, et al. The co-benefit of elemental mercury oxidation and slip ammonia abatement with SCR-Plus catalysts. Fuel 2014.
[7] Gong J, Ojifinni RA, Kim TS, White JM, Mullins CB. Selective catalytic oxidation of ammonia to nitrogen on atomic oxygen precovered Au (111). J Am Chem Soc 2006;128:9012–3.
[8] He C-Z, Wang H, Huai L-Y, Liu J-Y. Mechanism of ammonia decomposition and oxidation on Ir (100): a first-principles study. J Phys Chem C 2012;116:24035–45.
[9] Wang Q, Zhao B, Li G, Zhou R. Application of rare earth modified Zr-based ceria–zirconia solid solution in three-way catalyst for automotive emission control. Environ Sci Technol 2010;44:3870–5.
[10] Ko JH, Park SH, Jeon J-K, Kim S-S, Kim SC, Kim JM, et al. Low temperature selective catalytic reduction of NO with NH_3 over Mn supported on $Ce_{0.65}Zr_{0.35}O_2$ prepared by supercritical method: effect of Mn precursors on NO reduction. Catal Today 2012;185:290–5.
[11] Chen W, Ma Y, Qu Z, Liu Q, Huang W, Hu X, et al. Mechanism of the selective catalytic oxidation of slip ammonia over Ru-modified Ce–Zr complexes determined by in situ diffuse reflectance infrared fourier transform spectroscopy. Environ Sci Technol 2014;48:12199–205.
[12] Kameoka S, Suzuki T, Yuzaki K, Takeda T, Tanaka S, Ito S, et al. Selective catalytic reduction of N_2O with methane in the presence of excess oxygen over Fe-BEA zeolite. Chem Commun 2000:745–6.
[13] Zhang L, He H. Mechanism of selective catalytic oxidation of ammonia to nitrogen over Ag/Al_2O_3. J Catal 2009;268:18–25.
[14] van den Broek ACM. Low temperature oxidation of ammonia over platinum and iridium catalysts. Technische Universiteit Eindhoven; 1998.
[15] Yu T, Zeng J, Lim B, Xia Y. Aqueous-phase synthesis of Pt/CeO_2 hybrid nanostructures and their catalytic properties. Adv Mater 2010;22:5188–92.
[16] Ramis G, Yi L, Busca G. Ammonia activation over catalysts for the selective catalytic reduction of NO_x and the selective catalytic oxidation of NH_3. An FT-IR study. Catal Today 1996;28:373–80.
[17] Chen L, Li JH, Ge MF, Ma L, Chang HZ. Mechanism of selective catalytic reduction of NO_x with NH_3 over CeO_2–WO_3 catalysts. Chinese J Catal 2011;32:836–41.
[18] Matralis HK, Ciardelli M, Ruwet M, Grange P. Vanadia catalysts supported on mixed TiO_2–Al_2O_3 supports: effect of composition on the structure and acidity. J Catal 1995;157:368–79.
[19] Sun DK, Liu QY, Liu ZY, Gui GQ, Huang ZG. Adsorption and oxidation of NH_3 over V_2O_5/AC surface. Appl Catal B – Environ 2009;92:462–7.
[20] Zhou GY, Zhong BC, Wang WH, Guan XJ, Huang BC, Ye DQ, et al. In situ DRIFTS study of NO reduction by NH_3 over Fe–Ce–Mn/ZSM-5 catalysts. Catal Today 2011;175:157–63.
[21] Liu C, Ma Q, Liu Y, Ma J, He H. Synergistic reaction between SO_2 and NO_2 on mineral oxides: a potential formation pathway of sulfate aerosol. Phys Chem Chem Phys 2012;14:1668–76.
[22] Casapu M, Krocher O, Mehring M, Nachtegaal M, Borca C, Harfouche M, et al. Characterization of Nb-containing MnO_x–CeO_2 catalyst for low-temperature selective catalytic reduction of NO with NH_3. J Phys Chem C 2010;114:9791–801.
[23] Ramis G, Yi L, Busca G, Turco M, Kotur E, Willey RJ. Adsorption, activation, and oxidation of ammonia over SCR catalysts. J Catal 1995;157:523–35.
[24] Singh P, Mehrotra R, Bakhshi AK. Stress degradation studies of nelfinavir mesylate by Fourier transform infrared spectroscopy. J Pharmaceut Biomed 2010;53:287–94.
[25] Debeila MA, Coville NJ, Scurrell MS, Hearne GR. The effect of calcination temperature on the adsorption of nitric oxide on Au–TiO_2: drifts studies. Appl Catal A – Gen 2005;291:98–115.
[26] Liu FD, He H. Selective catalytic reduction of NO with NH_3 over manganese substituted iron titanate catalyst: reaction mechanism and H_2O/SO_2 inhibition mechanism study. Catal Today 2010;153:70–6.
[27] Qi G, Yang RT, Chang R. MnO_x–CeO_2 mixed oxides prepared by co-precipitation for selective catalytic reduction of NO with NH_3 at low temperatures. Appl Catal B 2004;51:93–106.
[28] Zawadzki J, Wiśniewski M. In situ characterization of interaction of ammonia with carbon surface in oxygen atmosphere. Carbon 2003;41:2257–67.
[29] Hadjiivanov KI. Identification of neutral and charged N_xO_y surface species by IR spectroscopy. Catal Rev 2000;42:71–144.
[30] Sun D, Liu Q, Liu Z, Gui G, Huang Z. Adsorption and oxidation of NH_3 over V_2O_5/AC surface. Appl Catal B 2009;92:462–7.

[31] Halkides TI, Kondarides DI, Verykios XE. Mechanistic study of the reduction of NO by C_3H_6 in the presence of oxygen over Rh/TiO_2 catalysts. Catal Today 2002;73:213–21.
[32] Koizumi N, Takahashi K, Yamazaki M, Yamada M. DRIFT study of temperature programmed desorption of NO adsorbed on $Co–Mo/Al_2O_3$ sulfided at high pressure. Catal Today 1998;45:313–8.
[33] Jiang B, Wu Z, Liu Y, Lee S, Ho W. DRIFT study of the SO_2 effect on low-temperature SCR reaction over $Fe–Mn/TiO_2$. J Phys Chem C 2010;114:4961–5.
[34] Liu F, Asakura K, He H, Shan W, Shi X, Zhang C. Influence of sulfation on iron titanate catalyst for the selective catalytic reduction of NO_x with NH_3. Appl Catal B 2011;103:369–77.
[35] Xu W, He H, Yu Y. Deactivation of a Ce/TiO_2 catalyst by SO_2 in the selective catalytic reduction of NO by NH_3. J Phys Chem C 2009;113:4426–32.
[36] Abdulhamid H, Fridell E, Dawody J, Skoglundh M. In situ FTIR study of SO_2 interaction with $Pt/BaCO_3/Al_2O_3$ NO_x storage catalysts under lean and rich conditions. J Catal 2006;241:200–10.